

# How to construct the most stable structure of (110) surface from rutile TiO<sub>2</sub> bulk?

Tran Thi Thoa<sup>1</sup>, Nguyen Trong Nghia<sup>2</sup>, Hoang Van Hung<sup>1</sup>, Nguyen Thi Minh Hue<sup>1,\*</sup>

<sup>1</sup>Faculty of Chemistry and Center for Computational Science, Hanoi National University of Education, 136 Xuan Thuy, Cau Giay, Ha Noi, Viet Nam

<sup>2</sup>School of Chemical Engineering, Hanoi University of Science and Technology, 1 Dai Co Viet, Hai Ba Trung, Ha Noi, Viet Nam

\*Emails: hue.nguyen@hnue.edu.vn

Received: 18 August 2022; Accepted for publication: 10 June 2023

**Abstract.** XRD pattern of rutile TiO<sub>2</sub> bulk and surface energy of possible terminated (110) planes were investigated using the DFT+U method. The (110) surface was demonstrated to be the most popular facet of rutile TiO<sub>2</sub>, which is in good agreement with the data of the JCPDS card No. 21-1276. The difference in surface energy among possible terminated (110) planes is attributed to the structure of the top and bottom atomic layers. We have found that the P5 plane is the most stable. It represents a structure of the (110) surface. The rutile TiO<sub>2</sub> (110) surface has a calculated surface energy of 0.98 J/m<sup>2</sup>. The value compares well with previous publications. Besides, DFT calculations were also performed. In comparison with DFT+U, the surface energy obtained from the DFT calculation for the (110) surface is very small, about 0.48 J/m<sup>2</sup>.

*Keywords:* XRD calculation, possible terminated (110) planes, surface energy, DFT+U, DFT.

*Classification numbers:* 2.2.2, 2.5.3.

## 1. INTRODUCTION

Fields of photocatalysis, photovoltaics, sensors, cosmetics, coating materials, and self-cleaning surfaces become extremely active thanks to the partial contribution of TiO<sub>2</sub>. This is a consequence of the semiconductor's interesting characteristics. TiO<sub>2</sub> has high chemical stability, abundance, low cost, high activity, strong oxidizing ability, corrosion resistance, nontoxicity, and biocompatibility [1]. TiO<sub>2</sub> naturally exists in three crystallographic phases: rutile, anatase, and brookite [2]. The thermodynamically most stable form at ambient conditions is rutile [3]. Rutile surfaces play an important role in the above applications. Various phenomena, such as catalytic activity, adsorption, and chemical interaction, take place on surfaces. The study on surfaces helps interpret properties and phenomena, and then design new materials. Before investigating surface properties, the construction of a surface from a bulk needs to be performed precisely. Any small mistake in this step leads to a series of errors in subsequent calculations on the surface. Therefore, the stage of creating a surface from bulk is crucial for studies on the surface. In calculations, the standard structure of a surface is a slab. A slab is an infinite two-

dimensional system standing for the facet of interest. The remaining dimension perpendicular to the facet is a vacuum. The vacuum height should be thick enough so that there is no interaction between adjacent slabs. Experiments indicated that the (110) surface is the most popular surface of rutile TiO<sub>2</sub> [4 - 5]. A question emerging is how to construct the surface from rutile TiO<sub>2</sub> bulk.

Strong electron correlation effects of *d* orbitals cause a challenge in theoretical studies on the structure and properties of rutile TiO<sub>2</sub> bulk as well as surfaces [6]. There are several solutions to the problem, in which DFT+U is one of the effective methods and has a reasonable computational cost. The value of Hubbard *U* affects the accuracy of the results from calculations on TiO<sub>2</sub> bulk and surfaces. Our previous publication demonstrated that the combination of *U<sub>d</sub>* and *U<sub>p</sub>* parameters enlarges the band gap and limits the deviation of lattice constants of TiO<sub>2</sub> bulk from the experiment [7]. We also showed that a (*U<sub>d</sub>* = 7 eV, *U<sub>p</sub>* = 10 eV) pair is one of the best choices for rutile TiO<sub>2</sub> bulk. How does the pair (*U<sub>d</sub>* = 7 eV, *U<sub>p</sub>* = 10 eV) affect the surface energy of the rutile TiO<sub>2</sub> (110) surface?

To provide insights into the details of how to build rutile TiO<sub>2</sub> (110) surface from bulk and the effect of the (*U<sub>d</sub>* = 7 eV, *U<sub>p</sub>* = 10 eV) pair on the surface energy, we have investigated rutile TiO<sub>2</sub> bulk and (110) surface. All calculations were implemented with the DFT+U approach. Firstly, we optimized the rutile bulk. The X-ray diffraction was then calculated to find the most popular surface of the rutile TiO<sub>2</sub>. From the relaxed bulk, we built possible (110) planes with different terminations. Finally, the energy surface was determined for each terminated (110) plane to find the most stable structure of the (110) surface. Besides, we carried out DFT calculations to compare with the results of the DFT+U calculations.

## 2. COMPUTATIONAL METHODS

All calculations were performed using the Vienna Ab initio Simulation Package (VASP) [8]. Perdew-Burke-Ernzerhof (PBE) functional within the generalized gradient approximation (GGA) was used to treat the exchange-correlation interaction [9-11]. Thresholds of 10<sup>-6</sup> eV and 0.01 eV Å<sup>-1</sup> were applied for energy and atomic force, respectively. The augmented-wave (PAW) approach was employed for core electrons. Meanwhile, valence electrons of Ti (3d<sup>2</sup>4s<sup>2</sup>) and oxygen (2s<sup>2</sup>2p<sup>4</sup>) were presented by plane waves with a cutoff energy of 450 eV [12]. In this paper, the DFT+U was performed in the formulation of Dudarev [13] with *U<sub>d</sub>* = 7 eV, *U<sub>p</sub>* = 10 eV and *J* = 0 eV. The Brillouin zone was sampled using 4 × 4 × 6 and 7 × 4 × 1 G-centered Monkhorst-Pack grids [14] for surface and bulk relaxations, respectively. A vacuum thickness of 12 Å was found to be enough to eliminate interaction between periodic images.

## 3. RESULTS AND DISCUSSION

### 3.1. The rutile TiO<sub>2</sub> bulk

Bulk rutile TiO<sub>2</sub> is tetragonal (*P4<sub>2</sub>/mnm*) with lattice constants *a*, *c*, and an internal parameter *u* standing for the distance between Ti and O atoms [15]. In the crystal, a Ti<sup>4+</sup> ion is surrounded by six O<sup>2-</sup> anions and each anion is surrounded by three Ti<sup>4+</sup> ions. The bulk is represented by a unit cell containing two Ti<sup>4+</sup> and four O<sup>2-</sup> ions. Bulk optimization using the DFT+U method yielded lattice constants *a* = 4.671 Å, *c* = 3.068 Å, and *u* = 0.305 Å, which were in line with the experimental results (*a* = 4.587 Å, *c* = 2.954 Å and *u* = 0.305 Å) [16]. In addition, the results from DOS calculations on the relaxed bulk demonstrated a bulk band gap of 2.92 eV, in good agreement with the experimental value [17].

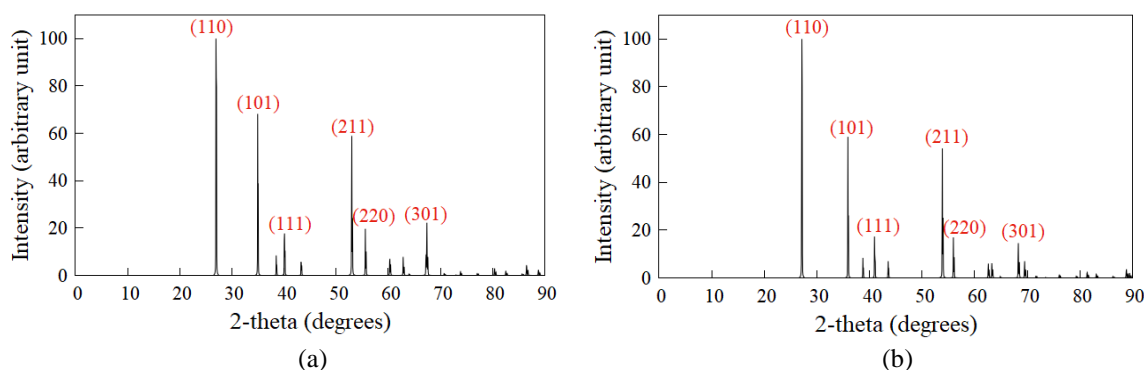


Figure 1. XRD patterns of rutile TiO<sub>2</sub> bulk from DFT+U (a) and DFT (b) calculations.

From the optimized structure of TiO<sub>2</sub> bulk, we calculated XRD patterns based on the DFT+U method. The results are shown in Fig. 1a. The XRD pattern exhibits strong diffraction peaks at the 2θ positions of 27.04°, 35.05°, and 53.13°. The peaks correspond to (110), (101), and (211) crystal surfaces, respectively. Besides, the pattern possesses peaks with low intensity, which stand for Miller indices of (111) at 2θ = 40.18°, (220) at 2θ = 55.75°, and (301) at 2θ = 67.58°. There is a good agreement between the calculated XRD pattern and the JCPDS card No. 21-1276 [5] (Table 1).

To compare with the results obtained from the DFT+U method, corresponding calculations were performed using the DFT method. The relaxed bulk has lattice constants  $a = 4.644 \text{ \AA}$ ,  $c = 2.966 \text{ \AA}$ , and  $u = 0.304 \text{ \AA}$ , closer to the experiment than the DFT+U calculations. However, the computed band gap from the DFT method is only 1.67 eV. The underestimation of the band gap is known as a disadvantage of the DFT approach in strongly correlated systems. The positions of primary peaks in the XRD pattern from the DFT calculation are shown in Table 1.

Table 1. Comparison of positions of main peaks in the XRD patterns obtained from DFT and DFT+U calculations.

Method	Plane	2-theta (2θ) (°)					
		(110)	(101)	(111)	(211)	(220)	(301)
DFT		27.2	35.99	41.07	53.99	56.10	68.48
DFT+U		27.04	35.05	40.18	53.13	55.75	67.58
Deviation		0.16	0.94	0.89	0.86	0.35	0.9
Exp. [5]		27.5	36.1	41.3	44.2	55.5	68.5

Here, deviation is defined as the difference in magnitude between the corresponding 2-theta angles from the two methods. The data in Table 1 indicate that the discrepancy in the XRD patterns is very small. The largest deviation is about 0.94°. The analysis of the two XRD patterns indicates that the (110) crystal plane is the most stable plane. Therefore, we chose the (110) plane for further study on surface.

### 3.2. Possible terminated (110) planes

Rutile TiO<sub>2</sub> (110) surface was built from relaxed bulk with bulk-terminated lattice constants in DFT+U calculation. It can be seen that there are six different kinds of termination for cutting (110) surface (Fig. 2. P1-a), which results in six terminated (110) planes. Each plane

corresponds to one atomic layer. The (110) planes are labeled as P1, P2, P3, P4, P5, and P6, respectively (Fig. 2). Here, the P1, P2, P4, and P5 planes are terminated with the dangling bond of oxygen, whereas the P3, P6 planes are terminated with dangling bonds of Ti<sub>2</sub>O<sub>2</sub> plane [18].

All (110) planes are in the forms of slabs with the same size as shown in Fig. 2. P1-b. Each slab consists of 4 trilayers in which atoms in the two bottom trilayers were fixed to their positions in the bulk. The total number of atoms in the slab is 24 atoms.

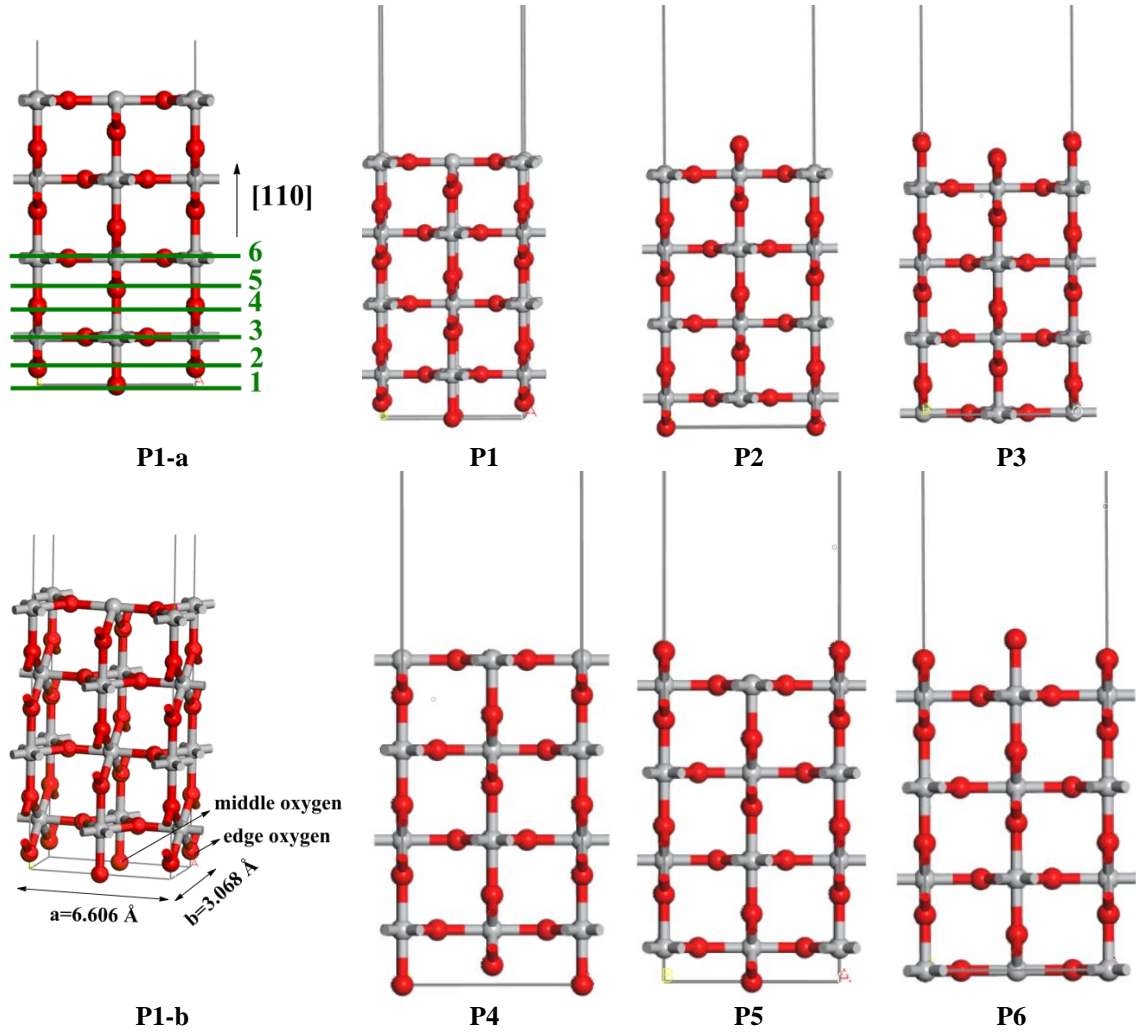


Figure 2. Possible terminated (110) planes.

To find the most stable structure of the (110) surface, we calculated the surface energy of all the possible terminated (110) planes. The difference in the total energy between the slab ( $E_{\text{slab}}$ ) and the bulk phase ( $E_{\text{bulk}}$ ) with the same number of TiO<sub>2</sub> units as the slab, divided by the total exposed area, is regarded as surface energy. Thus, the surface energy is revealed in the following expression:

$$E_{\text{surf}} = \frac{E_{\text{slab}}^{\text{no-rel}} - NE_{\text{bulk}}^{\text{rel}}}{2A} + \frac{E_{\text{slab}}^{\text{rel}} - E_{\text{slab}}^{\text{no-rel}}}{A}$$

here,  $E_{slab}^{rel}$ ,  $E_{bulk}^{rel}$  are the total energy of a slab and bulk unit cell after relaxation, respectively.  $E_{slab}^{no-rel}$  is the energy of the unrelaxed slab. The ratio of the number of atoms in the slab to those in bulk is  $N$ .  $A$  is the surface area of the slab. The factor of 2 presents that each slab contains two surfaces. The results of calculations on surface energy are summarized in Table 2.

Table 2. The surface energy of the possible terminated planes.

Plane	$E_{surf}(J / m^2)$		Plane	$E_{surf}(J / m^2)$
P1	2.91		P4	2.89
P2	1.00		P5	0.98
P3	3.35		P6	3.06

The smaller the surface energy, the more stable the plane. From Table 2, it can be seen that P5 has the lowest surface energy, about 0.98 J/m<sup>2</sup>, followed by the P2 plane, with 1.00 J/m<sup>2</sup>. The surface energy of the P6 and P3 planes is quite large, approximately 3.06 and 3.35 J/m<sup>2</sup>, respectively. Therefore, the P5 plane is the most stable plane. In other words, the P5 plane just represents the rutile (110) surface. The surface energy of the P5 plane may compare to previous studies using the DFT+U approach, 0.95 J/m<sup>2</sup> [19], 0.86 J/m<sup>2</sup> [20]. The surface energy of the possible (110) planes relates to their structures. The difference in structures comes mainly from the top and bottom atomic layers of each slab. The structures of these atomic layers of the six slabs are summarized in Table 3.

Table 3. Structures of the top and bottom atomic layers of slabs.

Plane (slab)	Ions in top atomic layer	Ions in bottom atomic layer
P1	Two Ti <sup>4+</sup> and two O <sup>2-</sup> ions	One O <sup>2-</sup> ion (middle oxygen)
P2	One O <sup>2-</sup> ion (middle oxygen)	One O <sup>2-</sup> ion (edge oxygen)
P3	One O <sup>2-</sup> ion (edge oxygen)	Two Ti <sup>4+</sup> and two O <sup>2-</sup> ions
P4	Two Ti <sup>4+</sup> and two O <sup>2-</sup> ions	One O <sup>2-</sup> ion (edge oxygen)
P5	One O <sup>2-</sup> ion (edge oxygen)	One O <sup>2-</sup> ion (middle oxygen)
P6	One O <sup>2-</sup> ion (middle oxygen)	Two Ti <sup>4+</sup> and two O <sup>2-</sup> ions

Examining the structure of the atomic layers of the slabs (Table 3) shows that P1 and P4 have similar structures: the top atomic layer contains two Ti<sup>4+</sup> and two O<sup>2-</sup> ions, and the bottom layer is composed of one O<sup>2-</sup> ion. The distinction between P1 and P4 is only one O<sup>2-</sup> ion in the bottom layer: one is middle oxygen, and one is edge oxygen. In the same way, P3 and P6 possess similar structures. By comparison, the top and bottom atomic layers of both P2 and P5 are O<sup>2-</sup> ions: one middle oxygen and one edge oxygen. We have three kinds of structural pairs: P1 and P4; P3 and P6; P2 and P5. Thanks to similar structures, the surface energy of (110) planes in each pair must be near. Indeed, as we can see in Table 2, the surface energy of P1 and P4 are 2.91 and 2.89 J/m<sup>2</sup>, respectively. Similarly, P2 and P5 have the surface energy of 1.00 and 0.98 J/m<sup>2</sup>, respectively. Values of 3.35 and 3.06 J/m<sup>2</sup> are the surface energy of P3 and P6, respectively.

In addition, we also performed DFT calculations on the surface energy of the P5' plane which corresponds to the P5 plane. The P5' plane was constructed from relaxation rutile TiO<sub>2</sub> bulk using the DFT calculation. Computed lattice constants of the P5' plane are  $a' = 6.497 \text{ \AA}$ ,  $b' = 2.959 \text{ \AA}$ . The energy surface of  $0.48 \text{ J/m}^2$  is demonstrated for the P5' plane. The value is consistent with other publications,  $0.5 \text{ J/m}^2$  [21],  $0.42 \text{ J/m}^2$  [22],  $0.4 \text{ J/m}^2$  [23], which could be compared with the experimental surface energy [24]. Therefore, in comparison with the DFT approach, the DFT+U method leads to an increase in surface energy of approximately two times.

#### 4. CONCLUSIONS

We examined rutile TiO<sub>2</sub> bulk and (110) surface using both DFT+U and DFT approaches. The procedures for determining the main facets of the bulk and the most stable structure of the (110) surface were shown in detail. XRD patterns from DFT+U and DFT calculations indicated the most popular facet of rutile TiO<sub>2</sub>. From relaxed bulk, possible (110) planes were constructed with different terminations. The results of the surface energy of all the possible (110) planes help to determine the most stable structure of the (110) surface. We also realized that both DFT+U and DFT methods give the same results of XRD, whereas the surface energy obtained from the DFT+U method for the (110) surface is twice that from the DFT method. We hope the present work provides useful and fundamental knowledge to know and understand how to determine the primary facets of bulk to construct and find out the most stable structure of a surface. The work is also expected to be the basis for further studies on surfaces.

**Acknowledgements.** We would like to thank the Hanoi National University of Education for providing a fruitful working environment.

**CRedit authorship contribution statement.** Nguyen Thi Minh Hue had scientific ideas, supervised and revised the manuscript. Hoang Van Hung supervised and revised the manuscript. Tran Thi Thoa and Nguyen Trong Nghia ran jobs and performed formal analysis of the results. All authors have read and agreed with the published version of the manuscript.

**Declaration of competing interest.** There are no conflicts to declare.

#### REFERENCES

1. Chen X. and Mao S. S. - Titanium Dioxide Nanomaterials: Synthesis, Properties, Modifications and Applications, *Chem. Rev.* **107** (7) (2007) 2891-2959.
2. Landmann M., Rauls E., and Schmidt W. G. - The electronic structure and optical response of rutile, anatase and brookite TiO<sub>2</sub>, *J. Phys.: Condens Matter* **24** (2012) 195503.
3. Li Y., Lee N. H., Lee E. G., Song J. S., Kim S. - The characterization and photocatalytic properties of mesoporous rutile TiO<sub>2</sub> powder synthesized through self-assembly of nano crystals, *Chem. Phys. Lett.* **389** (1-3) (2004) 124-128.
4. Sakurai K. and Mizusawa M. - X-ray Diffraction imaging of Anatase and Rutile, *Anal. Chem.* **82** (2010) 3519-3522.
5. Arami H., Mazloumi M., Khalifehzadeh R., Sadrnezhad S. K. - Sonochemical preparation of TiO<sub>2</sub> nanoparticle, *Mater. Lett.* **61** (23-24) (2007) 4559-4561.
6. Anisimov V. I., Poteryaev A. I., Korotin M. A., Anokhin A. O., and Kotliar G. - First-principles calculations of the electronic structure and spectra of strongly correlated systems: dynamical mean-field theory, *J. Phys. Condens. Matter* **9** (1997) 7359-7367.
7. Thoa T. T., Hung H. V., Hue N. T. M. - Study on structural and electronic properties of rutile TiO<sub>2</sub> using DFT+U approach, *Vietnam J. Chem.* **60** (2) (2022) 183-189.

8. <https://www.vasp.at/>
9. Perdew J. P., Burke K., and Ernzerhof M. - Generalized Gradient Approximation Made Simple, *Phys. Rev. Lett.* **77** (1996) 3865.
10. Perdew J. P., Burke K., and Ernzerhof M. - Generalized Gradient Approximation Made Simple, *Phys. Rev. Lett.* **78** (1997) 1396.
11. Perdew J. P., Burke K., and Ernzerhof M. - Generalized Gradient Approximation Made Simple, *Phys. Rev. Lett.* **80** (1998) 891.
12. Blochl P. E. - Projector augmented-wave method, *Phys. Rev. B* **50** (1994) 17953.
13. Dudarev S. L., Botton G. A., Savrasov S. Y., Humphreys C. J., Sutton A. P. - Electron-energy-loss spectra and the structural stability of nickel oxide: An LSDA+U study, *Phys. Rev. B* **44** (3) (1991) 943-954.
14. Pack H. J. M. A. J. D. - Special points for Brillouin-zone integrations, *Phys. Rev. B* **13** (1976) 5188.
15. Barbosaa M. A., Fabrisa G. S. L., Ferrera M. M., Azevedoa D. H. M., Sambrano J. R. - Computational Simulations of Morphological Transformations by Surface Structures: The Case of Rutile TiO<sub>2</sub> phase, *Materials Research* **20** (4) (2017) 920-925
16. Burdett J. K., Hughbanks T., Miller G. J., Richardson J. W., and Smith J. V. - Structural-Electronic Relationships in Inorganic Solids: Powder Neutron Diffraction Studies of the Rutile and Anatase Polymorphs of Titanium Dioxide at 15 and 295 K, *J. Am. Chem. Soc.* **109** (1987) 3639-3646.
17. Pascual J., Camassel J., and Mathieu H. - Fine structure in the intrinsic absorption edge of TiO<sub>2</sub>, *Phys. Rev. B* **18** (10) (1978) 5606-5614.
18. Hameeuw K. J., Cantele G., Ninno D., Trani F., Ladonisi G. - The rutile TiO<sub>2</sub> (110) surface: Obtaining converged structural properties from first – principles calculations, *J. Chem. Phys.* **124** (2006) 024708.
19. Cui Y., Yang K., Chen L., Liu B., Yang G., Gao Y. - Metal-insulator alternating behavior in VO<sub>2</sub>/TiO<sub>2</sub> supercells, *J. Alloys Compd.* **870** (2021) 159428.
20. Wallace S. K., Kenna K. P. M. - Facet Dependent Electron Trapping in TiO<sub>2</sub> Nanocrystals, *J. Phys. Chem. C* **119** (4) (2015) 1913-1920.
21. Perron H., Domain C., Roques J., Drot R., Simoni E., Catalette H. - Optimisation of accurate rutile TiO<sub>2</sub> (110), (100), (101) and (001) surface models from periodic DFT calculations, *Theor. Chem. Acc.* **117** (2007) 565-574.
22. Deringer V. L., and Csány G. - Many-Body Dispersion correlation effects on bulk and surface properties of rutile and Anatase TiO<sub>2</sub>, *J. Phys. Chem. C* **120** (38) (2016) 21552-21560.
23. Heckel W., Wurger T., Muller S., and Feldbauer G. - Van der Waals Interaction Really Matters: Energetics of Benzoic Acid on TiO<sub>2</sub> Rutile Surface, *J. Phys. Chem. C* **121** (32) (2017) 17207-17214.
24. Overbury S. H., Bertrand P. A., and Somorjai G. A. - The surface composition of binary systems. Prediction of surface phase diagrams of solid solution, *chem. Rev.* **75** (5) (1975) 547-560.